

PAPER • OPEN ACCESS

Crystal structure and optical properties of 1D-bi based organic-inorganic hybrid perovskite

To cite this article: Mohamed F. Kandeel *et al* 2019 *IOP Conf. Ser.: Mater. Sci. Eng.* **610** 012063

View the [article online](#) for updates and enhancements.

Recent citations

- [Synthesis, Characterization, and Optical Properties of New Organic-Inorganic Hybrid Perovskites \$\[\(NH_3\)_2\(CH_2\)_3\[CuCl_4\]\$ and \$\[\(NH_3\)_2\(CH_2\)_4\[CuCl_2Br_2\]\$](#)

Seham K. Abdel-Aal *et al*

- [Synthesis, crystal structure, Hirshfeld surface analysis, optical and antioxidant properties of the binuclear complex \$\[C_5H_{14}N_2I_2Bi_2Br_{10} \cdot 4H_2O\]\$](#)

Meriem El Ghali *et al*



240th ECS Meeting

Digital Meeting, Oct 10-14, 2021

We are going fully digital!

Attendees register for free!

REGISTER NOW



Crystal structure and optical properties of 1D-bi based organic-inorganic hybrid perovskite

Mohamed F.Kandeel^{1,3}, Seham K. Abdel-Aal^{2,4}, Ashraf F. El-Sherif^{1,5}, H. S. Ayoub^{2,6}, Ahmed S. Abdel-Rahman^{2,7}

¹ Laser and Photonics Center, Engineering Physics Department, Military Technical College, Cairo, Egypt.

² Physics department, Faculty of Science, Cairo University 12613, Cairo, Egypt.

Email: ³m.fawzy@mtc.edu.eg, ⁴seham@sci.cu.edu.eg, ⁵ashraf.alsharif@staff.aast.edu
⁶dr.hsayoub@gmail.com, ⁷asabry@sci.cu.edu.eg

Abstract. In the pages that follow, the structure of the crystal, unit cell dimension and complete structure information will be shown by single crystal x-ray diffraction and measuring some physical properties of 1D propylene diammonium pentachloro bismuthate $[(\text{NH}_3)_2(\text{CH}_2)_3]\text{BiCl}_5$ organic-inorganic hybrid perovskites (OIHs). Slow evaporation method is used to prepare the synthesis. The process of preparation occurred by mixing ethanolic solution of equimolar ratios (1:1) of its basic components (organic / inorganic). The Bi hybrid crystallized in orthorhombic non centro-symmetric Pca21 structure with 8 molecules per unit cell. The unit cell parameters are $a = 19.8403$ (7) Å, $b = 6.3303$ (2) Å, $c = 19.0314$ (7) Å. The average C-C bond lengths are 1.50 Å. The average N-C bond lengths are 1.47 Å. The connection between organic parts to inorganic part is via hydrogen bond (H. Bond). Raman spectroscopy and also Fourier transform infrared spectroscopy (FTIR) have been used to study the vibrational spectra that shows the main diffraction peaks and their assignment. Diffuse reflectance spectra (DRS) method is used to study the optical properties and show that there is a strong absorption in the UV region for Bi hybrid. Kubelka–Munk equation has been used to calculate the band gap energy and indicates that the band gap for the present investigated hybrid is equals 3.15 eV

Keywords: 1D-2D hybrid perovskite; Bi halide perovskite; optical properties

1. Introduction

Organic-inorganic hybrid perovskites (OIHs) are very promising class of new materials. It possesses exceptional structural and properties tunability. The dimensionality also can be tuned according to the chemical formula, coordination geometry of the metal ion and the valence of organic cation. 3D-general formula AMX_3 [1, 2], 2D- A_2MX_4 [3, 4] and 1D- A_2MX_5 [5, 6] where the organic cation is A, metal ion is M, halide is X can be Cl, Br or I. Structures on the molecular scale all are possible. OIHs have been widely studied due to their potentially useful properties including tunable bandgap [4, 7, 8], long exciton and charge diffusion lengths [9, 10], high extinction coefficient [11, 12], which make these materials have potential applications in various optoelectronic devices, ranging from photovoltaic cells (PVs) [2], to light emitting diodes (LEDs) [1].



Noteworthy progress are observed to OIHs recently but research has been focus mainly on 3D and 2D[1, 13] structures, with 1D and 0D structures significantly underexplored. Regarding this issue, in this work we will focus on 1D perovskites based on Bi ion. Its structure have the $[\text{BiX}_6]^{4-}$ octahedrons connected in a chain by edges or faces or corner shared surrounded by organic cations, which allows to form bulk assemblies of 1D quantum confined materials. The unique structure allows interesting photophysical properties [4, 14]. In this work the single crystal x-ray diffraction of 1, 2 diammonium penta-chloro bismuthate $[(\text{NH}_3)_2(\text{CH}_2)_3]\text{BiCl}_5$ is presented. The prepared crystal is grown from solution by slow evaporation process. Crystallographic information and unit cell dimensions as well as selected bond distances and bond angles are provided. The organic cation and inorganic anion are connected via H bond between the H of ammonia group of organic part and the chloride ion of the Bismuth chloride of inorganic part.

2. Experimental

2.1. Synthesis.

The chemicals used in the preparation process are from SIGMA-ALDRICH and used as received. The purity is exceeding 99%. Solvents were of reagent grade. The organic cation 1, 2 di-ammonium propane-chlorate $[(\text{NH}_3)_2(\text{CH}_2)_3]\text{Cl}_2$ synthesized by adding a drops of 30 % HCl to 4 gm 1,2-diaminopropan dissolved in 100 ml ethanol and placed in an ice bath till pH~4. The resulting solution is heated to 60°C for 0.5 hour under constant stirring. Colorless needle crystals of $[(\text{NH}_3)_2(\text{CH}_2)_3]\text{Cl}_2$ precipitate out upon gradual cooling to room temperature.

The crystals filtered and dried then kept in vacuum desiccator until use. Perovskite hybrid of $[(\text{NH}_3)_2(\text{CH}_2)_3]\text{BiCl}_5$ was prepared by mixing 1 M of ethanolic solution of both $[(\text{NH}_3)_2(\text{CH}_2)_3]\text{Cl}_2$ and BiCl_3 in 1:1 stoichiometric ratio (organic/ inorganic), under constant stirring, heat to 60 °C for 30 min followed by slow cooling to room temperature in a double wall container. Colorless cubic crystals of $[(\text{NH}_3)_2(\text{CH}_2)_3]\text{BiCl}_5$ precipitate out. The reaction proceeds according to equation (1).



Good untwined not cracked crystals are selected for single crystal X-ray measurements. The carbon, nitrogen, hydrogen percentage have been determined by Microchemical analyses, Table 1 show there is a good agreement between found and calculated percentages.

Table1. The chemical analysis of $[(\text{NH}_3)_2(\text{CH}_2)_3]\text{BiCl}_5$

Element	Found	Calculated
C%	7.80	8.01
H%	2.38	2.49
N%	6.00	5.21

2.2. Characterization.

2.2.1. Raman and IR Spectroscopy

An FTIR 4100 spectrometer using pure KBr pellets has been used to obtain the FTIR spectra between 4000-400 cm^{-1} . For Raman spectra a high power stabilizer laser (Ocean optics inc., model 5116), Peak wave length was 785 nm, and output power > 350 mW, High resolution spectrometer (Ocean Optics inc., model QE5000) with detector range from UV to NIR (200-1100 nm). Raman coupled fiber probe for 785 nm with SMA connector of 7.5 mm OD (Ocean Optics Inc., Model RPB 785).

2.2.2. Crystal structure

The single crystal X-ray crystallographic data were collected on Crys Alis Pro 1.171.38.41 (Rigaku Oxford Diffraction, 2015) Empirical absorption correction using spherical harmonics, implemented in SCALE3 ABSPACK scaling algorithm. Reflections were merged by SHELXL according to the crystal class for the calculation of statistics and refinement. Hg and DIAMOND programs have been used to prepare the graphics.

2.2.3. Optical properties

The room temperature at which absorption diffuse reflectance spectrum and the UV–Vis were recorded. Then UV–Vis–NIR spectro-photometer type Jasco-V-570 spectrophotometer, Japan, fitted with integrating sphere reflectance unit (ISN) has been used to collect the data in the wavelength range 200 to 2000 nm.

3. Result and discussion

3.1. Structure description.

Metal halide perovskite hybrids could be assembled using varieties of organic and inorganic components. Basic building blocks are (metal halide octahedrons, MX_6 according to the coordination geometry of metal ion, where M is a metal and X is a halogen). And the organic part which may be functional alkyl chains or heterocyclic aromatic. These varieties in the structure enabled the metal halide perovskites to be arranged in different ways exhibiting 3D, 2D, and 1D structure as said in the introduction section.

The structure of presently investigated organic-inorganic perovskite hybrid of 1, 2 diammonium penta-chloro bismuthate $[(NH_3)_2(CH_2)_3]BiCl_5$ in the 3D view consists of 8 molecules per unit cell. The organic di-cations $[(NH_3)_2(CH_2)_3]^{2+}$ and inorganic di-anions $[BiCl_5]^{2-}$ are distributed in unit cell. Figures 1.a , 1.b and 1.c show the view of the molecule in c direction , in the unit cell in 3D view and H. bond network marked by dashed line of $[(NH_3)_2(CH_2)_3]BiCl_5$ along b plan. Table 2 Crystallographic information, unit cell parameters and refinement of $[(NH_3)_2(CH_2)_3]BiCl_5$.

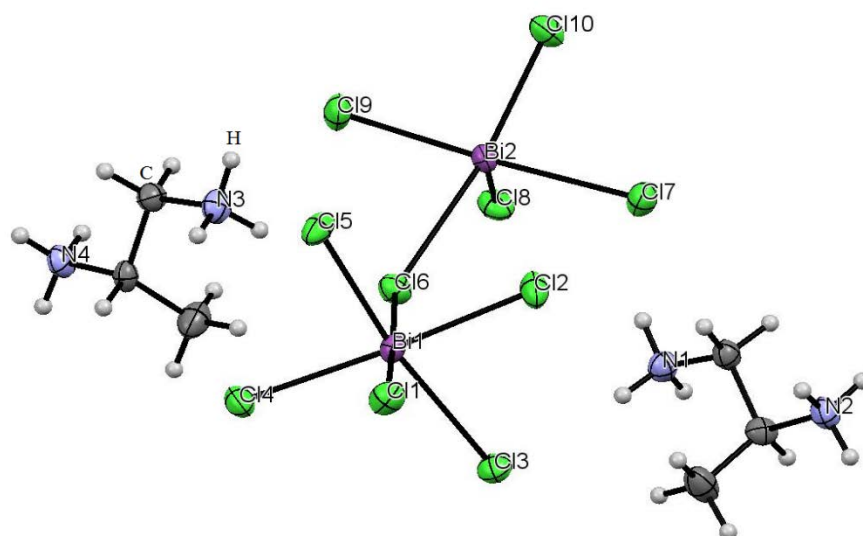


Figure 1(a) View of the $[(NH_3)_2(CH_2)_3]BiCl_5$ molecule in c direction

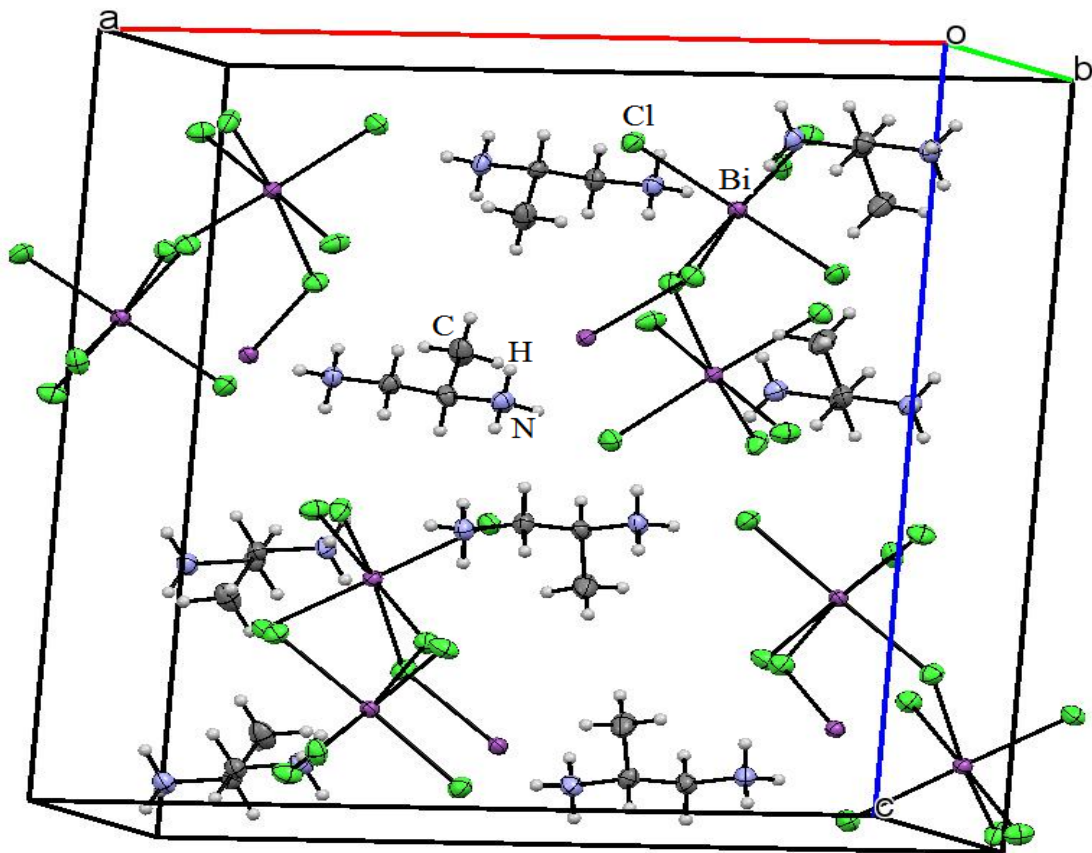


Figure 1(b) Arrangement of the $[(\text{NH}_3)_2(\text{CH}_2)_3]\text{BiCl}_5$ in the unit cell in 3D view

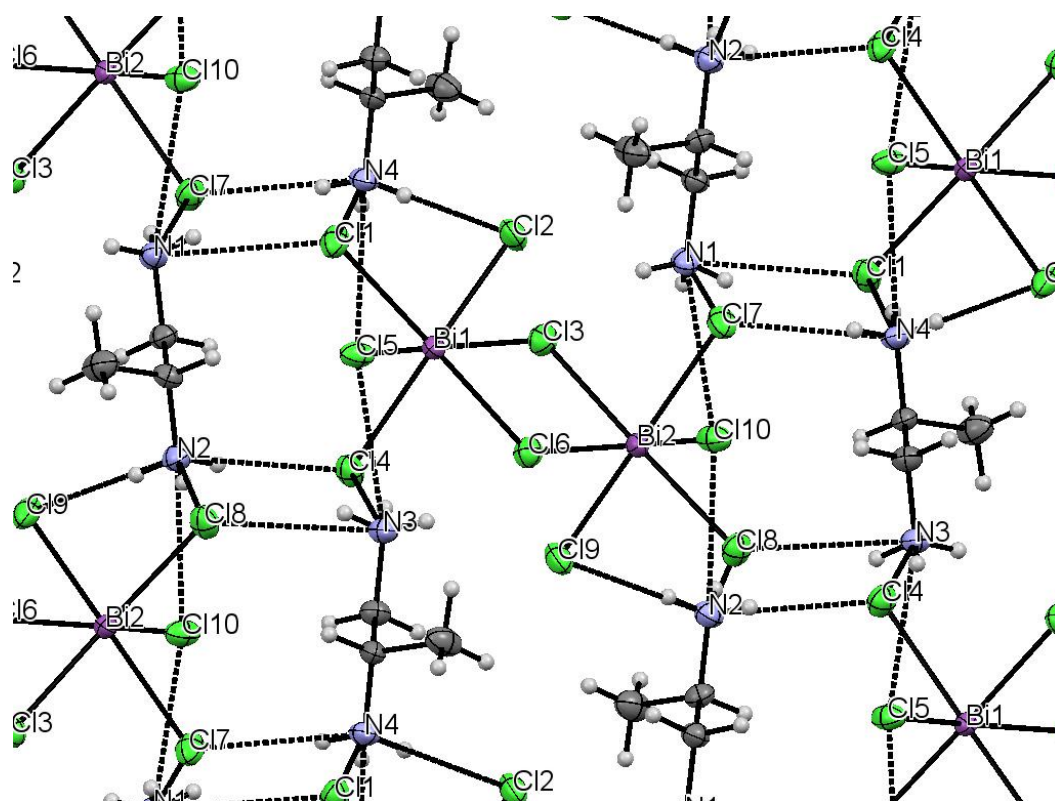


Figure 1(c) H. bond network marked by dashed line of $[(\text{NH}_3)_2(\text{CH}_2)_3]\text{BiCl}_5$ along b plan

The coordination geometry of the Bi atoms show a highly distorted octahedron formed by C11, C12, C13, C14, C15 for Bi1 and C16, C17, C18, C19, C10, for Bi2 atom. The Bi-Cl bond distances are ranged from 2.555 Å to 2.929 Å with an average of 2.722 Å. The Cl-Bi-Cl angles are varies from 82.13° to 176.94° that deviate from ideal octahedral structure values (90° and 180°). The average values of the distortion parameters of $[\text{BiCl}_5]^{2-}$ is calculated using equation (2), (3) [15].

$$ID(\text{Bi} - \text{Cl}) = \frac{1}{nD_{\text{avg}}} \sum_{i=1}^n |D_i - D_{\text{avg}}|, n = 10 \quad (2)$$

$$ID(\text{Cl} - \text{Bi} - \text{Cl}) = \frac{1}{mA_{\text{avg}}} \sum_{j=1}^m |A_j - A_{\text{avg}}|, m = 20 \quad (3)$$

where D is the (Bi-Cl) bond distances, A is the (Cl-Bi-Cl) bond angles, D_{avg} and A_{avg} are the average values of bond distances and bond angles respectively. The values of the distortion indices are $ID(\text{Bi-Cl}) = 0.039$ for bond distances and $ID(\text{Cl-Bi-Cl}) = 0.24$ for bond angles. The high distortion indices may be attributed to the large size of Bi^{3+} ion in the octahedron.

The organic part contain 2 molecule per asymmetric unit of $[(\text{NH}_3)_2(\text{CH}_2)_3]^{2+}$ the two NH_3 attached at adjacent two carbon atoms and in the trans position this is to decrease the steric hindrance. The average C-C bond lengths are 1.50 Å. The average N-C bond lengths are 1.47 Å. These values are in good agreement with bond lengths of other previously studied diammonium salts [3, 16, 17] [18, 19]. Table 3 lists selected bond length (Å), bond angles (°) and dihedral angles. The structure is stabilized by hydrogen bonding H. bond between Cl⁻ anion of inorganic part $[\text{BiCl}_5]^{2-}$ and the H-atoms of NH_3 at organic part $[(\text{NH}_3)_2(\text{CH}_2)_3]^{2+}$ cation. Table 4 shows the H. bond geometry.

Table 2. Crystallographic information, unit cell parameters and refinement of $[(\text{NH}_3)_2(\text{CH}_2)_3]\text{BiCl}_5$

Empirical formula	$\text{C}_3 \text{H}_{12} \text{N}_2, \text{Bi Cl}_5$
M_r	462.38
Crystal color, shape	Transparent, cube
Space group	Orthorhombic
	$P c a 2_1$
a	19.8403(7) Å
b	6.3303(2) Å
c	19.0314(7) Å
α, β, γ	90°
V	2390.25 Å ³
Z	8
D_x	2.570 Mg m ⁻³
Radiation type	Mo $K\alpha$
λ	0.71073 Å
θ_{max}	34.99 °
μ	2.303 mm ⁻¹
T	242 K
Shape	Cubic
Color	Clear white

Table 3. Selected bond distances [Å] and angles [°] of $[(\text{NH}_3)_2(\text{CH}_2)_3]\text{BiCl}_5$ Crystal

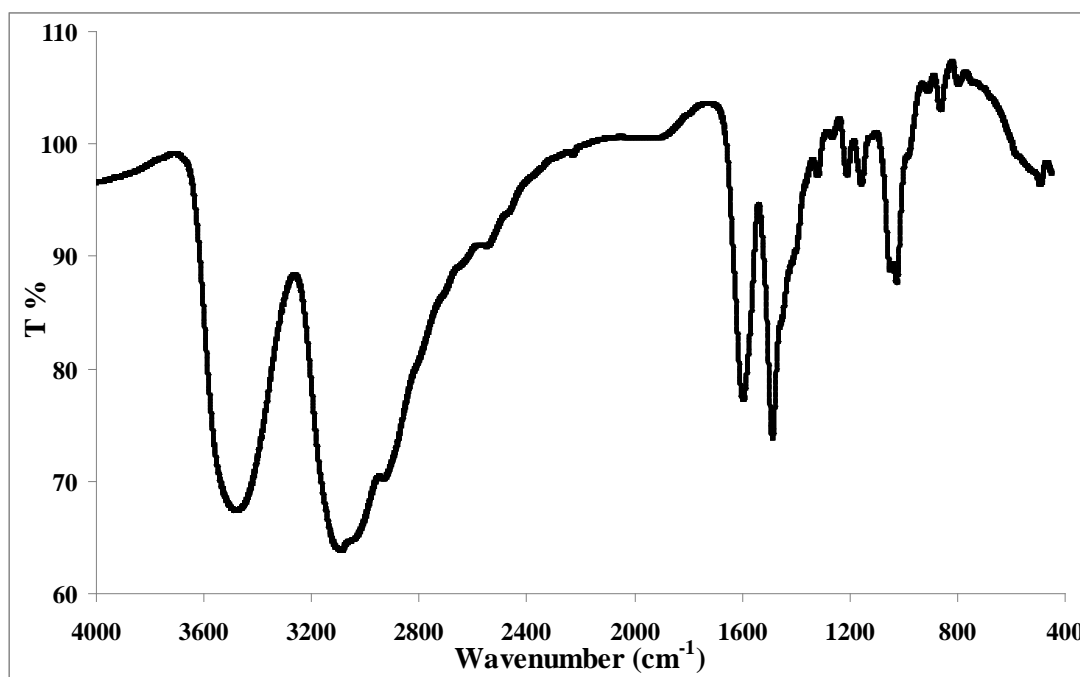
Octahedron BiCl_6			
Distances (Å)		Angles (°)	
$\text{Bi}_1\text{-Cl}_1$	2.721	$\text{Cl}_1\text{-Bi}_1\text{-Cl}_2$	85.32
$\text{Bi}_1\text{-Cl}_2$	2.629	$\text{Cl}_1\text{-Bi}_1\text{-Cl}_3$	100.31
$\text{Bi}_1\text{-Cl}_3$	2.925	$\text{Cl}_1\text{-Bi}_1\text{-Cl}_4$	98.52
$\text{Bi}_1\text{-Cl}_4$	2.789	$\text{Cl}_1\text{-Bi}_1\text{-Cl}_5$	86.24
$\text{Bi}_1\text{-Cl}_5$	2.555	$\text{Cl}_2\text{-Bi}_1\text{-Cl}_3$	82.13
$\text{Bi}_2\text{-Cl}_6$	2.929	$\text{Cl}_2\text{-Bi}_1\text{-Cl}_4$	176.65
$\text{Bi}_2\text{-Cl}_7$	2.783	$\text{Cl}_2\text{-Bi}_1\text{-Cl}_5$	92.00
$\text{Bi}_2\text{-Cl}_8$	2.712	$\text{Cl}_3\text{-Bi}_1\text{-Cl}_4$	100.26
$\text{Bi}_2\text{-Cl}_9$	2.632	$\text{Cl}_3\text{-Bi}_1\text{-Cl}_5$	170.76
$\text{Bi}_2\text{-Cl}_{10}$	2.548	$\text{Cl}_4\text{-Bi}_1\text{-Cl}_5$	85.33
		$\text{Cl}_6\text{-Bi}_2\text{-Cl}_7$	108.41
		$\text{Cl}_6\text{-Bi}_2\text{-Cl}_8$	99.80
		$\text{Cl}_6\text{-Bi}_2\text{-Cl}_9$	82.08
		$\text{Cl}_6\text{-Bi}_2\text{-Cl}_{10}$	170.75
		$\text{Cl}_7\text{-Bi}_2\text{-Cl}_8$	95.49
		$\text{Cl}_7\text{-Bi}_2\text{-Cl}_9$	176.94
		$\text{Cl}_7\text{-Bi}_2\text{-Cl}_{10}$	85.18
		$\text{Cl}_8\text{-Bi}_2\text{-Cl}_9$	85.79
		$\text{Cl}_8\text{-Bi}_2\text{-Cl}_{10}$	86.89
		$\text{Cl}_9\text{-Bi}_2\text{-Cl}_{10}$	92.12

Table 4. The H- bond geometry of hybrid perovskite $[(\text{NH}_3)_2(\text{CH}_2)_3]\text{BiCl}_5$, Donor atom D =N, Acceptor atom A =Cl

(D-H-A)	d (D-H) (Å)	D (H-A) (Å)	< (D-H-A) (°)	d (D-A) (Å)
N1—H1B—C11	0.901	2.543	136.89	3.260
N1—H1A—C17	0.900	2.313	157.84	3.166
N1—H1C—C110	0.899	3.260	80.90	3.242
N2—H2A—C14	0.900	2.973	164.10	3.161
N2—H7C—C110i	0.900	2.920	97.22	3.162
N2—H2B—C19	0.900	2.382	178.58	3.281
N3—H3D—C14i	0.900	2.336	160.47	3.198
N3—H3E—C18	0.900	2.514	141.74	3.268
N3—H3F—C15	0.901	3.230	80.82	3.211
N4—H4A—C17i	0.900	2.393	140.07	3.137
N4—H4C—C11i	0.900	2.345	163.97	3.220
N4—H4B—C12	0.900	2.371	177.51	3.271

3.2. Vibrational spectroscopy.

Vibrational study using infrared absorption and Raman scattering has been carried out to gain more information on the crystal structure. The infrared and Raman spectra at room temperature are shown in Fig. 2 and Fig. 3 respectively.

**Figure 2.** The Infrared spectrum of the compound $[(\text{NH}_3)_2(\text{CH}_2)_3]\text{BiCl}_5$ at room temperature

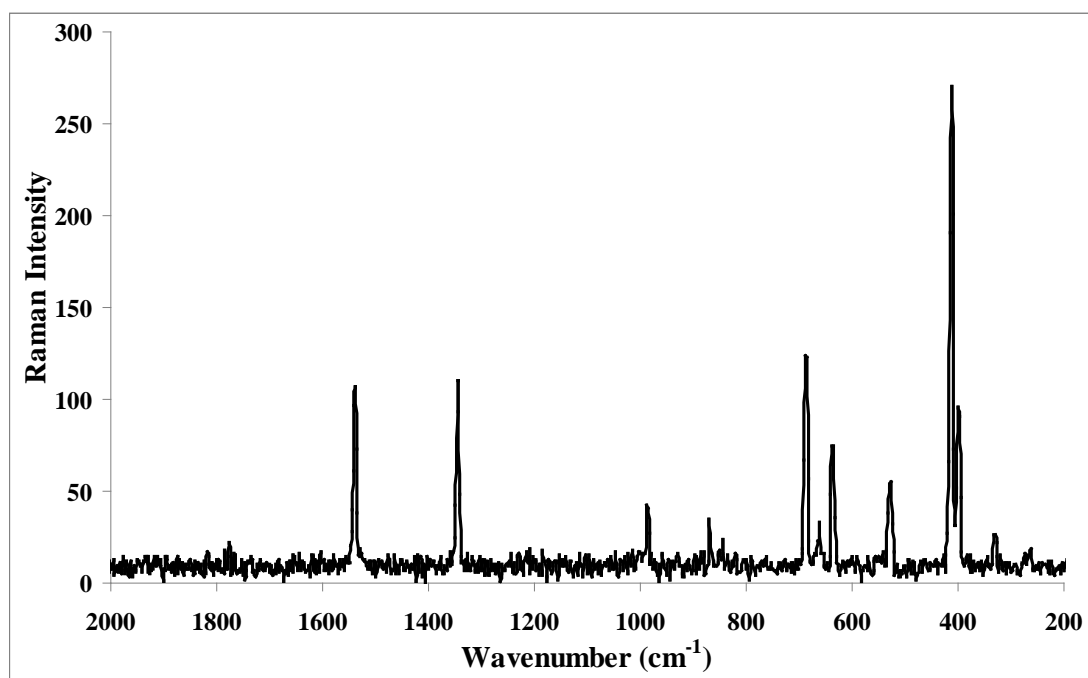


Figure 3. Raman spectrum of $[(\text{NH}_3)_2(\text{CH}_2)_3]\text{BiCl}_5$ at room temperature

According to crystal structural results, the prepared hybrid corresponds to $\text{Pca}2_1$ space group, C_{2v} character table and point group $\text{mm}2$. The vibrational modes in C_{2v} character table which consists of A_1 , A_2 , B_1 and B_2 representations are IR and Raman active except the representation A_2 display only Raman.

A detailed assignment of all bands observed in the infrared and Raman spectra of $[\text{NH}_3(\text{CH}_2)_3\text{NH}_3]\text{BiCl}_5$ is not rigorously possible and such assignment might be meaningless since the part of the spectra corresponding to the bands assigned to the stretching, bending, rocking, twisting and wagging modes of the methyl groups is very complex.. The assignment of the observed bands is given in Table 5. It was based, on the one hand, on results obtained previously 1, 2, 3 and 4, on the other hand, on the group factor analysis.

Table 5. The assignment of the observed bands of IR and Raman for the compound $[\text{NH}_3(\text{CH}_2)_3\text{NH}_3]\text{BiCl}_5$

Raman bands ^a	IR bands ^a	Assignment	Ref
209vw		$\nu(\text{Bi-Cl})$ Bridge	[20]
240vw		$\nu(\text{Bi-Cl})$ External and Bridging	[15], [20]
274vw		$\nu(\text{Bi-Cl})$ Terminal	[15], [20]
	400m	-	
	412vs	-	
437vw		$\Delta(\text{C-N})$	[12]
493vw	493w	-	

526w	520vw	$\Delta(\text{N-H})$	[12]
688m	706vw	-	
798vw	798w	$\text{P}(\text{CH}_2)$, $\rho(\text{NH}_3)$	[15]
834vw		$\text{P}(\text{NH}_3)$	[15]
869vw	862m	$\nu_{\text{sy}}(\text{C-N})$	[15]
914vw	911w	$\nu_{\text{sy}}(\text{C-N})$, $\beta(\text{C-H})$	[15]– [12]
938vw		$\Delta(\text{C-H})$, $\rho(\text{NH}_3)$	[15]–[12]
957vw		$\Delta(\text{C-C})$	[20]
987w		$\nu_{\text{asy}}(\text{C-N})$, $\nu_{\text{sy}}(\text{C-C})$	[15]– [12]
1022vw	1026s	$\nu_{\text{asy}}(\text{C-N})$	[15]
1033vw		$\nu_{\text{sy}}(\text{C-C})$	[12, 21]
1045vw	1050s	$\beta(\text{C-H})$, $\nu_{\text{sy}}(\text{C-N})$	[12, 21]
1076vw		$\nu_{\text{sy}}(\text{C-C})$	[15], [20, 21]
1123vw	1123vw	$\nu_{\text{sy}}(\text{C-N})$	[21]
1161vw	1159m	$\nu_{\text{sy}}(\text{C-N})$, $\rho(\text{NH}_3)$	[15], [20]–[21]
1183vw		$\text{P}(\text{NH}_3)$	[15]
1203vw		$\nu_{\text{sy}}(\text{C-N})$	[12]
1215vw	1212m	$\nu_{\text{sy}}(\text{C-C})$	[12]
1267w	1268vw	$\delta(\text{CH}_2)$ twisting, $\nu_{\text{s}}(\text{C-N})$	[15]
1303vw		$\delta(\text{CH}_2)$ twisting	[15]
1329vw	1321m	$\delta(\text{CH}_2)$ twisting/wagging	[15]
1344m		$\nu_{\text{asy}}(\text{C-C})$	[20]
1403vw		$\delta(\text{CH}_2)$ wagging	[15]
1451vw		$\delta(\text{CH}_2)$ scissoring	[15]
1464vw		$\delta(\text{CH}_2)$ scissoring	[15, 20]
1489vw	1487vs	$\delta_{\text{sy}}(\text{CH}_3)$, $\delta(\text{C-H})$	[12, 15]
1538vw		$\nu_{\text{sy}}(\text{C-N})$	[12]
1598vw	1596vs	$\delta(\text{NH}_2)$, $\delta_{\text{asy}}(\text{CH}_3)$, $\delta(\text{C-H})$	[15, 20]
	2933s	$\nu_{\text{asy}}(\text{CH}_2)$, $\nu_{\text{sy}}(\text{N-H})$	[15] [12]
	3092vs	$\nu_{\text{sy}}(\text{NH}_2)$, $\nu_{\text{sy}}(\text{NH}_3)$	[15]–[20]
	3481vs	$\nu_{\text{asy}}(\text{NH}_2)$	[12]– [21]

^avw: very weak ,w: weak ,m: medium ,s: strong ,vs: very strong.

^bsy: symmetric ,asy: asymmetric ,v: stretching , δ : scissoring, β : in plane bending

3.3. Internal modes of the $^+\text{NH}_3(\text{CH}_2)_3\text{NH}_3^+$ cation.

The free cation contains 17 atoms and was assumed to have the C_1 symmetry where Nitrogen atoms are attached to Carbon atoms #1 and #2 as shown in Figure 4. Thus, its 45 internal modes of vibration are assigned to the A mode and thus they are IR and Raman active.

The principal bands are assigned to the internal modes of organic cation. In fact, the high-frequency intense region $1489\text{--}3481\text{ cm}^{-1}$ is related to the symmetric, asymmetric stretching and bending vibrations of NH, NH_2 , NH_3 , CH, CH_2 , CH_3 and CN. The medium and thin band observed at 1267 and 1464 cm^{-1} is associated to organic carbon chain different bending modes. The band observed at 437 and 1215 cm^{-1} mainly corresponds to atom to atom vibrations in the organic chain.

The anion part of the molecule vibrations are observed in the range 209 to 274 cm^{-1} and caused by Bi-Cl stretching.

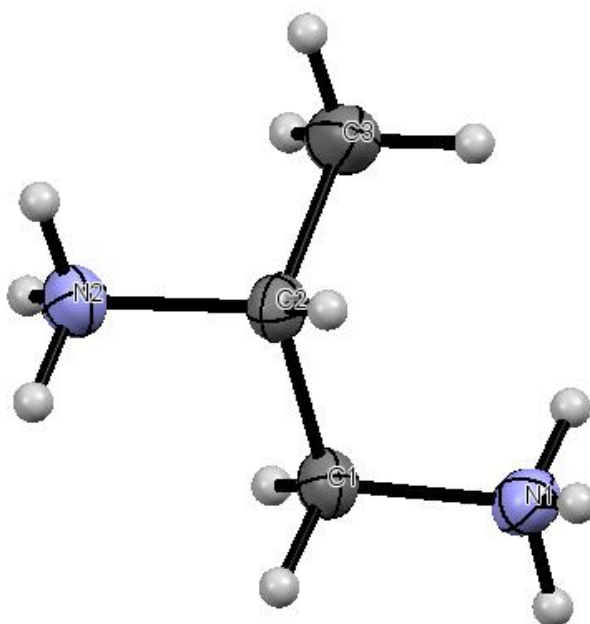


Figure 4. The structure of the $^+\text{NH}_3(\text{CH}_2)_3\text{NH}_3^+$ cation.

3.4. Optical measurements.

Diffuse reflectance spectra (DRS) is a spectroscopic technique based on the reflection of light in the ultraviolet, visible, and near infrared regions by a fine powdered sample. In this technique the ratios of light scattered from a thick sheet of investigated sample and reference sample from an ideal non absorbing material is measured as a function of the wavelength λ (i.e. $F_{\text{SKM}}(R_\infty)$ vs. λ nm). The Schuster- Kubelka- Munk (SKM) remission function has been used to correlate the relation between the diffuse reflectance of the sample (R_∞), absorption (K) and scattering (S) coefficients.

$$F_{\text{SKM}}(R_\infty) = \frac{(1-R_\infty)^2}{2R_\infty} = \frac{K}{S} \quad (4)$$

By extrapolating the straight line plot of $(F(R_\infty) h\nu)^n$ versus $(h\nu)$ from optical reflectance spectra the energy gap E_g is determined according to the following Kubelka-Munk equation.

$$(F(R_{\infty})h\nu)^n = A(h\nu - E_g) \quad (5)$$

Where ν is the frequency of vibration, h is the Plank's constant, A is a constant and E_g is band gap. According to the type of transition the exponent n can be $n = 1/2$ or $3/2$ for indirect transitions, but for direct allowed transitions is 2 or 3 [20, 22-26]. Figure 5 demonstrates the optical properties of the present investigated perovskite hybrid. In the uv region the sample has a strong absorption shown by the optical properties and the estimated energy gap energy is equals to 3.2 eV. The spectra exhibit two distinct absorptions bands at 218 nm and 370 nm. That may attribute to the Metal Centered (MC) transition from the 6s to 6s 6p of Bismuth atom. The band at 218 nm can be assigned to ligand, to metal charge transfer (LMCT) transition from the 5p orbital of Cl to 6p orbital of Bi(III) as reported before[25].

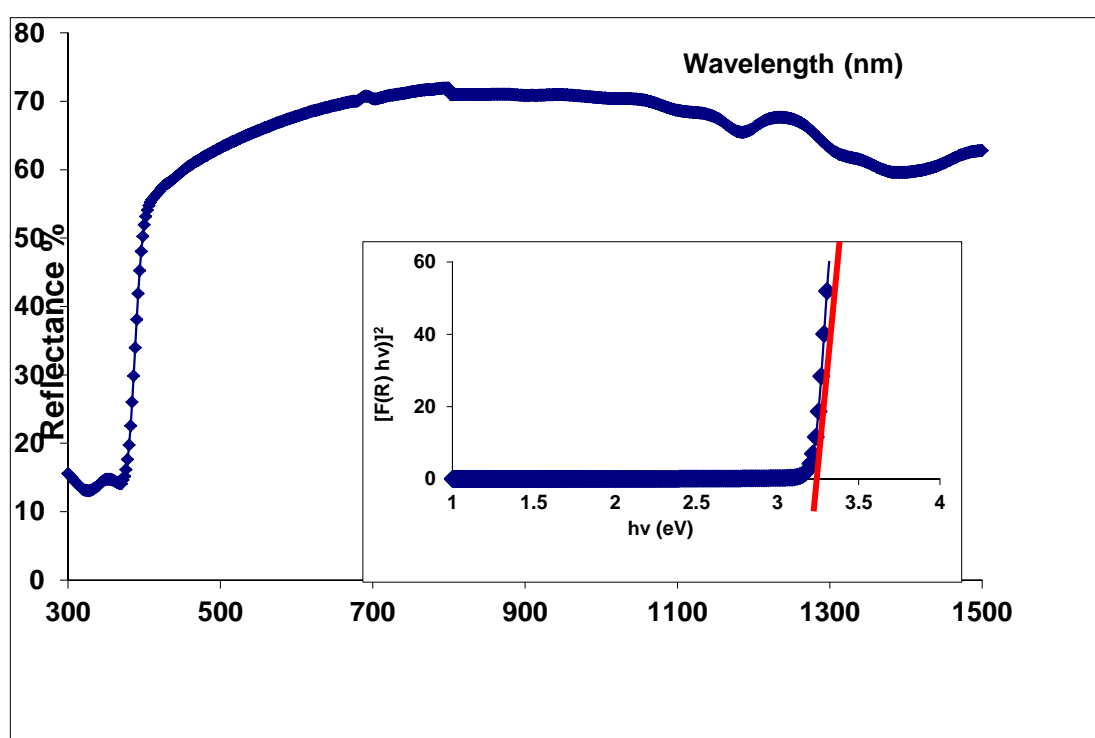


Figure 5. diffused reflectance of $[\text{NH}_3(\text{CH}_2)_3\text{NH}_3]\text{BiCl}_5$, the inset fig represent the band gap energy value

4. Conclusion

1, 2 diammonium penta-chloro bismuthate $[(\text{NH}_3)_2(\text{CH}_2)_3]\text{BiCl}_5$ is successfully prepared by evaporation method from ethanolic solution. This hybrid perovskite crystallized in an orthorhombic system space group $\text{Pca}2_1$ noncentrosymmetric with unit cell parameters are $a = 19.8403(7) \text{ \AA}$, $b = 6.3303(2) \text{ \AA}$, $c = 19.0314(7) \text{ \AA}$, $\alpha = \beta = \gamma = 90^\circ$. H. Bond connect organic and inorganic components. The characteristic vibrational peaks clearly appear in FTIR and Raman spectroscopy. A strong absorption has been shown by the optical properties in the uv region, its band gap energy 3.15 eV.

References

- [1] Q. Chen *et al.*, "Under the spotlight: The organic–inorganic hybrid halide perovskite for optoelectronic applications," *Nano Today*, vol. 10, no. 3, pp. 355-396, 2015.
- [2] Z. Cheng and J. Lin, "Layered organic–inorganic hybrid perovskites: structure, optical properties, film preparation, patterning and templating engineering," *CrystEngComm*, vol. 12, no. 10, pp. 2646-2662, 2010.
- [3] M. Mostafa, S. S. El-khiyami, and S. Alal, "Structure, thermal, and impedance study of a new organic–inorganic hybrid [(CH₂)₇(NH₃)₂]CoCl₄," *Journal of Physics and Chemistry of Solids*, vol. 118, pp. 6-13, 2018.
- [4] W. Bi, N. Leblanc, N. Mercier, P. Auban-Senzier, and C. Pasquier, "Thermally induced Bi (III) lone pair stereoactivity: ferroelectric phase transition and semiconducting properties of (MV)BiBr₅ (MV= methylviologen)," *Chemistry of Materials*, vol. 21, no. 18, pp. 4099-4101, 2009.
- [5] D. Fredj *et al.*, "Structural, vibrational and optical properties of a new organic–inorganic material:(C₅H₈N₃)₂[BiCl₅]," *Materials Research Bulletin*, vol. 85, pp. 23-29, 2017.
- [6] J. H. Noh, S. H. Im, J. H. Heo, T. N. Mandal, and S. I. Seok, "Chemical management for colorful, efficient, and stable inorganic–organic hybrid nanostructured solar cells," *Nano letters*, vol. 13, no. 4, pp. 1764-1769, 2013.
- [7] G. E. Eperon, S. D. Stranks, C. Menelaou, M. B. Johnston, L. M. Herz, and H. J. Snaith, "Formamidinium lead trihalide: a broadly tunable perovskite for efficient planar heterojunction solar cells," *Energy & Environmental Science*, vol. 7, no. 3, pp. 982-988, 2014.
- [8] S. D. Stranks *et al.*, "Electron-hole diffusion lengths exceeding 1 micrometer in an organometal trihalide perovskite absorber," *Science*, vol. 342, no. 6156, pp. 341-344, 2013.
- [9] G. Xing *et al.*, "Long-range balanced electron-and hole-transport lengths in organic-inorganic CH₃NH₃PbI₃," *Science*, vol. 342, no. 6156, pp. 344-347, 2013.
- [10] J.-H. Im, C.-R. Lee, J.-W. Lee, S.-W. Park, and N.-G. Park, "6.5% efficient perovskite quantum-dot-sensitized solar cell," *Nanoscale*, vol. 3, no. 10, pp. 4088-4093, 2011.
- [11] H.-S. Kim *et al.*, "Lead iodide perovskite sensitized all-solid-state submicron thin film mesoscopic solar cell with efficiency exceeding 9%," *Scientific reports*, vol. 2, p. 591, 2012.
- [12] M. S. Lassoued *et al.*, "Synthesis, crystal structure, vibrational spectroscopy and photoluminescence of new hybrid compound containing chlorate anions of stanate (II)," *Journal of Molecular Structure*, vol. 1141, pp. 660-667, 2017.
- [13] S. K. Abdel-Aal, G. Kocher-Oberlehner, A. Ionov, and R. Mozhchil, "Effect of organic chain length on structure, electronic composition, lattice potential energy, and optical properties of 2D hybrid perovskites [(NH₃)(CH₂)_n(NH₃)]CuCl₄, n= 2–9," *Applied Physics A*, vol. 123, no. 8, p. 531, 2017.
- [14] H. Dammak, S. Triki, A. Mlayah, Y. Abid, and H. Feki, "Structural, vibrational and optical properties of a new self assembled organic–inorganic nanowire crystal (C₆H₁₄N)₂[BiBr₅]. A Density Functional Theory approach," *Journal of Luminescence*, vol. 166, pp. 180-186, 2015.
- [15] H. Jeghnou *et al.*, "Structural phase transition in [NH₃(CH₂)₅NH₃]BiCl₅: thermal and vibrational studies," *Journal of Raman Spectroscopy: An International Journal for Original Work in all Aspects of Raman Spectroscopy, Including Higher Order Processes, and also Brillouin and Rayleigh Scattering*, vol. 36, no. 11, pp. 1023-1028, 2005.
- [16] S. K. Abdel-Aal and A. S. Abdel-Rahman, "Synthesis, structure, lattice energy and enthalpy of 2D hybrid perovskite [NH₃(CH₂)₄NH₃]CoCl₄, compared to [NH₃(CH₂)_nNH₃]CoCl₄, n= 3–9," *Journal of Crystal Growth*, vol. 457, pp. 282-288, 2017.
- [17] M. F. Mostafa, S. S. El-Khiyami, and S. K. Abd-Elal, "Crystal structure, phase transition and conductivity study of two new organic–inorganic hybrids:[(CH₂)₇(NH₃)₂]X₂, X= Cl/Br," *Journal of Molecular Structure*, vol. 1127, pp. 59-73, 2017.

- [18] P. Mondal, S. K. Abdel-Aal, D. Das, and S. M. Islam, "Catalytic Activity of Crystallographically Characterized Organic–Inorganic Hybrid Containing 1, 5-Di-amino-pentane Tetrachloro Manganate with Perovskite Type Structure," *Catalysis Letters*, vol. 147, no. 9, pp. 2332-2339, 2017.
- [19] M. F. Mostafa, S. S. Elkhiyami, and S. A. Alal, "Discontinuous transition from insulator to semiconductor induced by phase change of the new organic-inorganic hybrid [(CH₂)₇(NH₃)₂]CoBr₄," *Materials Chemistry and Physics*, vol. 199, pp. 454-463, 2017.
- [20] H. Ferjani and H. Boughzala, "New Quasi-One-Dimensional Organic-Inorganic Hybrid Material: 1, 3-Bis (4-piperidinium) propane Pentachlorobismuthate (III) Synthesis, Crystal Structure, and Spectroscopic Studies," *Journal of Materials*, vol. 2014, 2014.
- [21] M. Essid, Z. Aloui, M. Rzaigui, and H. Marouani, "Synthesis, crystal structure and IR spectroscopy of a new 2-methylpiperazine-1, 4-dium pentachlorobismuthate (III) monohydrate:[C₅H₁₄N₂]BiCl₅·H₂O," *Journal: Journal of Advances in Chemistry*, vol. 10, no. 4.
- [22] C. Xiao *et al.*, "Mechanisms of electron-beam-induced damage in perovskite thin films revealed by cathodoluminescence spectroscopy," *The Journal of Physical Chemistry C*, vol. 119, no. 48, pp. 26904-26911, 2015.
- [23] A. Vogler and H. Nikol, "The Structures of s₂ metal complexes in the ground and sp excited states," *Comments on Inorganic Chemistry*, vol. 14, no. 4, pp. 245-261, 1993.
- [24] H. Nikol and A. Vogler, "Photoluminescence of antimony (III) and bismuth (III) chloride complexes in solution," *Journal of the American Chemical Society*, vol. 113, no. 23, pp. 8988-8990, 1991.
- [25] H. Nikol, A. Becht, and A. Vogler, "Photoluminescence of germanium (II), tin (II), and lead (II) chloride complexes in solution," *Inorganic Chemistry*, vol. 31, no. 15, pp. 3277-3279, 1992.
- [26] A. Vogler and H. Nikol, "Photochemistry and photophysics of coordination compounds of the main group metals," *Pure and applied chemistry*, vol. 64, no. 9, pp. 1311-1317, 1992.